# Hydrogen Generation in a Reverse-Flow Microreactor: 2. Simulation and Analysis

**Niket S. Kaisare and Jay H. Lee**
School of Chemical and Biomolecular Engineering, Georgia Institute of Technology, Atlanta, GA 30332

**Andrei G. Fedorov**
Woodruff School of Mechanical Engineering, Georgia Institute of Technology, Atlanta, GA 30332

*DOI 10.1002/aic.10493*
*Published online May 19, 2005 in Wiley InterScience (www.interscience.wiley.com).*

*The second part in this series presents parametric simulation and sensitivity analysis of methane partial oxidation in a microreactor operated with periodic flow reversal. The reverse-flow (RF) operation provides up to a 5% increase in the hydrogen yield compared to that of the unidirectional (UD) operation. The effect of varying the inlet $CH_4$:$O_2$ feed ratio, the inlet velocity, and the inlet gas temperature is studied. The optimal feed ratio is found to be $CH_4$:$O_2$ = 1.15:1 with the feed at ambient room temperature. The effects of varying the reactor length and heat losses to the ambient are also investigated. In both these cases, the performance of the UD operation degrades significantly, whereas the performance of the RF operation is more robust to the variations in reactor size and heat losses. The issue of choosing the optimal switching time is also addressed. Switching the input and output ports near the natural timescale of reaction heat release is shown to provide the optimum yield. Through these results, design and operation guidelines based on simple timescale analysis have emerged.* © 2005 American Institute of Chemical Engineers
*AIChE J,* 51: 2265–2272, 2005
*Keywords: reactor analysis, simulation, process, hydrocarbon processing*

## Introduction

Forced unsteady-state operation (see Matros[1] for an excellent review) of chemical reactors and separation processes often lead to an improved performance over the steady-state operation. For example, Horn and Lin[2] used a variational approach to determine the optimal periodic operation of a CSTR. Horn[3] showed an improvement in efficiency of a periodically operated separation processes. Sterman and Ydstie[4,5] used the so-called pi-criterion to analyze the feasibility of a periodic operation. Bailey[6] used convex set theory for optimization in periodic control. Eigenberger and Nieken[7] examined combustion of volatile organics at low concentrations in reverse-flow reactors (RFRs), whereas Haynes et al.[8] proposed a procedure for the design of RFRs. The last two cited examples involve operating a reactor in a reverse-flow (RF) mode through periodic switching of the input and output ports, resulting in a reversal of the flow direction. Matros and Bunimovich[9] provide a comprehensive review of theoretical and experimental developments in RFRs. The RF operation often leads to transient patterns in a catalytic system that are not found in the steady-state operation. The opportunity for improvement in the performance of a RFR occurs as a result of dynamic properties on the catalyst and/or the dynamic properties of the whole reactor.[10]

In this work, partial oxidation of methane in a reverse-flow microreactor is considered. Previous work on the RF operation of methane partial oxidation has mostly focused on fixed-bed reactors or catalytic monoliths. Blanks et al.[11] were among the first to provide experimental and simulation studies on a pilot-

Correspondence concerning this article should be addressed either to J. H. Lee at jay.lee@che.gatech.edu or to A. G. Fedorov at andrei.fedorov@me.gatech.edu.

scale RFR for methane partial oxidation. de Groote et al.[12] showed that a thermal wave is formed in a fixed-bed partial oxidation reactor, which travels along the length of the reactor. They showed that this traveling wave in the RFR goes through three different stages in each semicycle: the wave development stage, wave widening stage, and the wave propagation stage. Gosiewski and coworkers compared the performance of the RFR[13] with a unidirectional reactor with periodic feed cycling.[14] Fissore et al.[15] used their model for simulation of periodic changing of feed location in a three-reactor network to vary the sequence of reactors.

Modeling of methane partial oxidation for autothermal operation of a microreactor running in the unidirectional (UD) and reverse-flow (RF) modes and an analysis of timescales of individual processes occurring within the reactor were presented in the first article of this two-part series.[16] Using the reaction kinetics adapted from Gosiewski et al.,[13] we were able to reproduce the experimental result of Kikas et al.[17] that the RF operation of the reactor provides a higher hydrogen yield and a lower maximum temperature compared to those of the UD operation of the microreactor. In this report, we use timescale analysis to obtain the origins of the observed improvement in the performance with the RF operation. Because the reaction and diffusion timescales are very fast, species concentrations reach a quasi-steady state. Therefore, the dynamic thermal properties of the entire reactor can be exploited to obtain process intensification in the RF operation of the microreactor. Specifically, the RF operation may result in one or more of the following advantages[9]:

- Creating conditions that are thermodynamically favorable for reversible reactions
- Efficient energy use, resulting in a more uniform temperature pattern, consequently resulting in better performance at a smaller reactor size and lower average reactor temperature
- Using the RFR as a regenerative heat exchanger that allows the autothermal operation of weakly exothermic processes

These three benefits are highlighted in Figure 1. Figures 1a–1c show the schematic of temperature profiles for three different situations in the UD operation, whereas Figure 1d shows the corresponding temperature profile for the RF operation. Figure 1a shows the case in which an autothermal UD state is obtained and the reactor is long enough for the desired reaction to reach equilibrium. The gas exits the reactor at a relatively high temperature, which is thermodynamically unfavorable for an exothermic reaction. In the RF operation, however, the sharp drop in the temperature at the reactor exit provides a thermodynamically favorable condition, shifting the equilibrium toward the desired product. A similar trend is also observed in an RFR with high-temperature feed for an endothermic reversible reaction. The second case (Figure 1b) is usually found when endothermic and exothermic reactions are coupled and the reactions do not reach equilibrium within the reactor. The temperature decreases on either side of the hot spot in the UD operation, resulting in lower rates of reactions and a poor use of the reactor. In an RFR, flanged between the two hot spots near the reactor ends is an extended region of high temperature. The rates of endothermic reactions are high in this region. Consequently, the conversion and yield of the desired product are also higher. The third and perhaps the most widely studied example is that of a slightly exothermic high-temperature reaction, which is unable to provide sufficient heat to maintain the UD steady state. In such a situation, a traveling wave is usually formed. The RFR is then used as a regenerative heat exchanger, trapping the thermal wave within the reactor by flow reversal before the reaction front exits the reactor.

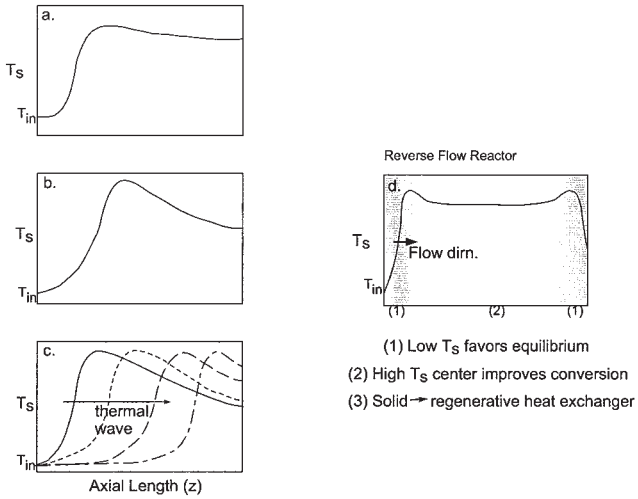


**Figure 1. Temperature profiles in UD operation for three possible conditions: (a) reactions proceed to equilibrium, (b) poor utilization of reactor, (c) thermal wave travels and exits the reactor.**

In the RF operation (d), there is an extended region (2) of high temperature where reactions reach equilibrium flanged between the shaded regions (1) of thermodynamically favorable conditions at reactor ends.

The rest of the paper is organized as follows. The simulation results are presented in the next section. The effects of changing the $CH_4$:$O_2$ feed ratio, the presence of water in the feed, and the variations in velocity or gas temperature at the inlet are studied. We also consider the effect of reactor length and the reactor heat losses on the reactor performance. The analysis of the RF operation is presented in the analysis section. All three circumstances for process intensification mentioned in the previous paragraph were observed for different conditions in the simulated reactor and are discussed in this section. The effect of varying the switching time is studied and guidelines for optimal reactor operation based on the scale analysis are presented. Finally, the key findings are summarized in the concluding section.

## Simulation Results

### *Adiabatic reactor: base case*

The "base case" refers to simulations of the adiabatic reactor for the parameters used in the experiments.[17] These are summarized in Table 1 of Part 1 of this series,[16] and simulation results were presented therein. The reactor consists of four channels, 500 microns in diameter and 11.6 cm in length. In this section, simulation results for varying input conditions for the reactor in the unidirectional (UD) and reverse-flow (RF) operation are discussed.

*Inlet Feed Concentrations.* The effect of varying feed ratios $CH_4$:$O_2$ is shown in Table 1 and in Figure 2. As the feed ratio $CH_4$:$O_2$ is increased, the selectivity to hydrogen increased, resulting in an increase in hydrogen yield. This hap-

**Table 1. Simulations of the Reactor Performance for Various Inlet Feed Ratios**

| | | Unidirectional | | Reverse-Flow | | |
|---|---|---|---|---|---|---|
| Case | $CH_4$:$O_2$ Ratio | $T_{s,\max}$ | %$H_2$ Yield | $T_{s,\max}$ | $T_{s,\text{out}}$ | %$H_2$ Yield |
| 1 | 0.7:1 | 2160 | 57.3 | 2023 | 1280 | 61.5 |
| 2 | 1:1 | 2008 | 71.1 | 1880 | 1191 | 73.4 |
| 3 | 1.15:1 | 1951 | 77.5 | 1816 | 1132 | 77.4 |
| 4 | 1.25:1 | 1914 | 77.0 | 1779 | 1093 | 76.6 |
| 5 | 1.5:1 | 1841 | 74.4* | 1703 | 1007 | 72.6 |
| 6 | 1.75:1 | tw | tw | 1660 | 939 | 65.2 |
| 7 | 2:1 | tw | tw | 1608 | 890 | 59.2 |

*Note:* A traveling thermal wave is formed at a feed ratio of 1.5:1 and higher.
* The wave creeps through the reactor, and the reported hydrogen yield is that obtained for >2 h of operation. tw, traveling wave; no UD autothermal state is observed.

pened until the $CH_4$:$O_2$ ratio reached 1.15:1. Beyond this point, the hydrogen yield decreased again and an optimal feed ratio was found to be $CH_4$:$O_2$ = 1.15:1. This compares favorably with the experimentally reported optimal ratio of about 0.9:1.[17] This is a departure from the published literature,[12,13] where a ratio closer to the partial oxidation ($CH_4 + 0.5O_2 \rightleftharpoons CO + 2H_2$) stoichiometric ratio of 2:1 is generally used. A maximum improvement of 4% in hydrogen yield in the RF over UD operation was observed at $CH_4$:$O_2$ = 0.7:1. Additionally, at $CH_4$:$O_2$ feed ratios of 1.25:1 and higher, the model predicted lower hydrogen yield in the RF operation compared to that in the UD operation. A slowly creeping thermal wave was observed for $CH_4$:$O_2$ = 1.5:1. Because of the low speed of wave propagation within the reactor, a stable UD operation was possible for 2–3 h before the reactor quenched. Finally, with water present in the feed, autothermal UD operation was not obtained. In contrast, at lower amounts of water in the feed, autothermal RF operation was possible, although there was a decrease in the hydrogen yield. A further increase in the amount of water resulted in the complete disappearance of autothermal operation, even in the RF operation of the reactor.

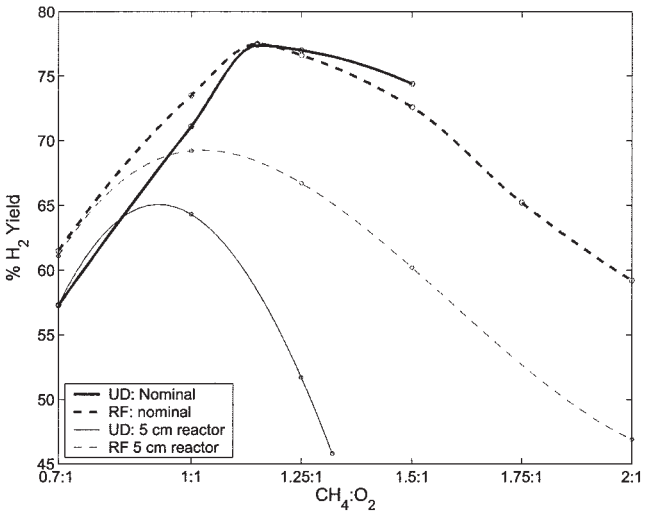


**Figure 2. Comparison of the UD (—) and RF (– –) operations for various $CH_4$:$O_2$ ratios for the nominal reactor (thick lines) and the shorter 5-cm reactor (thin lines). Also see Table 1.**

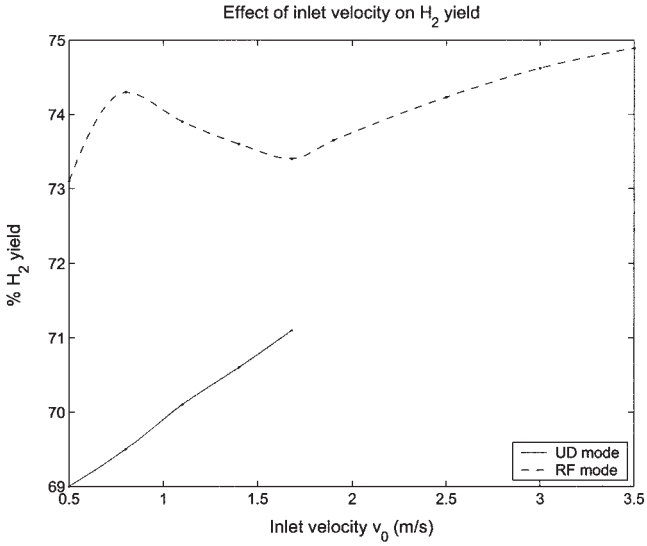


**Figure 3. Effect of varying inlet velocity on $H_2$ yield.**

Autothermal UD state cannot be obtained for $v_0$ = 1.8 m/s or higher.

These results are consistent with those observed experimentally.[17]

*Influence of the Inlet Velocity.* Figure 3 shows the variation in hydrogen yield in the UD and RF operations with the inlet velocity for constant feed ratio of $CH_4$:$O_2$ = 1:1 and inlet gas temperature $T_{g0}$ = 300 K. Changing the velocity had a substantial effect on the reactor performance. In the UD operation, hydrogen yield showed almost a linear dependency on the inlet velocity. Increasing the velocity to 1.8 m/s resulted in the formation of a thermal wave and the autothermal UD steady state disappeared. When the inlet velocity was increased further, the speed of propagation of the thermal wave increased almost linearly with the inlet velocity. On the other hand, even when the velocity was decreased to 0.5 m/s, the movement of the reaction front opposite to the direction of the flow (flash back) was not observed.

The effect of inlet velocity on the RF operation was quite different. Increasing $v_0$ resulted in a decrease in hydrogen yield until about 1.8 m/s. Recall that this is the point where thermal wave was formed in the UD operation. When the inlet velocity for the RF operation was increased beyond this point, the hydrogen yield also increased and finally reached a "saturation" at $v_0 \approx 3.5$ m/s. The effect of velocity on solid temperature (not shown) in the UD and RF operations was more predictable: increasing the inlet velocity resulted in a monotonic increase in the solid temperature as a result of higher throughput of the reactants through the microreactor. Consequently, for low velocities (such as $v_0 < 0.75$ m/s), overall conversion to hydrogen in the RF operation dropped as a result of lower peak temperatures.

*Influence of the Inlet Gas Temperature.* The effect of varying the inlet gas temperature on the UD operation, as shown in Figure 4 for a constant inlet velocity $v_0$ = 1.68 m/s, was less significant than that of the inlet velocity. Hydrogen yield decreased slightly with an increase in $T_{g0}$ in both the UD and RF operations; however, the hydrogen yield in the RF operation decreased more noticeably than that in the UD operation.

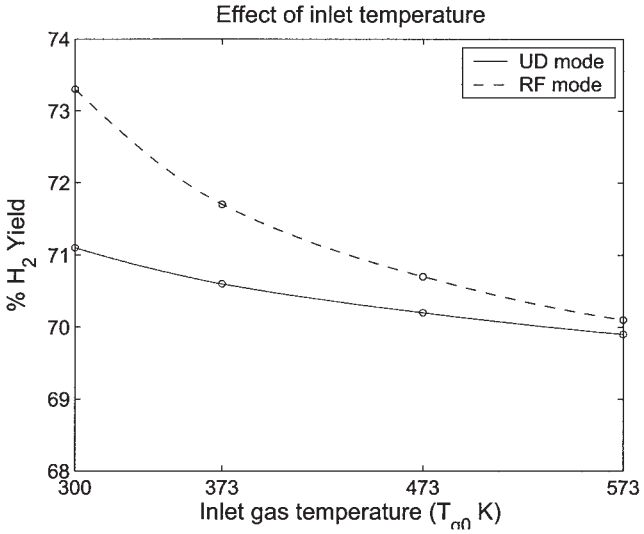


**Figure 4. Effect of varying inlet gas temperature ($T_{g0}$) for $v_0$ = 1.68 m/s and $CH_4$:$O_2$ = 1:1 on hydrogen yield.**

$H_2$ yield decreases as the inlet temperature increases.

Around $T_{g0}$ = 573 K, the RF operation provided little improvement over the UD operation (Figure 4). In addition to this, increasing the $T_{g0}$ had the effect of stabilizing the traveling thermal wave; in fact, when $T_{g0}$ was increased to 573 K, an autothermal UD steady state was observed for $CH_4$:$O_2$ = 2:1 with inlet velocity of $v_0$ = 1.68 m/s.

### *Effect of reactor length*

The effect of varying the reactor length was studied by comparing the results obtained for the 11.6-cm-long reactor in the previous section with those for a 5-cm-long reactor. The aspect ratio *l*/*d* for this reactor is 100, compared to *l*/*d* = 232 for the nominal reactor. The dashed line in Figure 2 shows the performance of the 5-cm-long reactor in the UD and RF operations. This case is interesting because the reactor length is insufficient for the reactions to attain equilibrium. Thus, the hydrogen yield for the UD operation is much lower for the 5-cm reactor compared to that of the longer reactor. The optimum feed ratio also changed: for the UD operation of the shorter reactor, $CH_4$:$O_2 \approx 0.9$:1 was optimal. It is interesting to note that the improvement in the performance for RF over UD operation was greater in the shorter 5-cm reactor. For the entire range of feed conditions, the RF operation provided much better hydrogen yield than the UD operation for this shorter reactor. Unlike the UD operation, the optimum feed ratio for the RF operation did not change much from that found in the long (base case) reactor (that is, optimal $CH_4$:$O_2 \approx 1.1$:1).

### *Effect of heat losses*

As mentioned earlier, the reactor is housed in a steel casing and is covered with a Ni–Cr coil for preheating the reactor. It is then covered with a thick layer of insulation and a layer of radiation shield. The heat losses were thus very low and adiabatic reactor assumption is a good approximation. However, heat losses are vital issues in a microreactor operation. Thus, we simulate a case wherein the reactor is poorly insulated. We account for resistance to external heat transfer, resistance of steel casing, air gap between the steel casing and the reactor tube, and the ceramic reactor tube itself. In such a situation, the heat-transfer coefficient was estimated as approximately 6.2 W $m^{-2}$ $K^{-1}$. In this situation, the reactor did not maintain autothermal operation for the UD mode. However, the autothermal operation was maintained in the RF mode. The pertinent results are given in Table 2. This is a significant result because it shows that the RF operation is a robust method for on-demand generation of hydrogen even in the presence of large heat losses.

## Analysis of the Reverse-Flow Operation

In this section, we attempt to provide plausible explanations of process intensification in a microreactor under the RF operation over UD operation. Because the reaction and diffusion timescales are fast, the reactor operation is governed by the thermal dynamics of the microreactor. The timescale of reaction heat release ($\tau_{Hrxn}$ = 3.2 s) and the timescale of thermal relaxation of a volume element of the reactor ($\tau_{th}$ = 168 s) are critical parameters that provide approximate handles for selection of switching time $\tau_{c/2}$. There are three different possibilities for selecting the switching time:

(1) switching faster than time of heat release by reaction ($\tau_{c/2} \leq \tau_{Hrxn}$)

(2) switching slower than the thermal relaxation timescale ($\tau_{c/2} \geq \tau_{th}$)

(3) switching between the two timescales ($\tau_{Hrxn} < \tau_{c/2} < \tau_{th}$)

As mentioned earlier and in Figure 1, we consider three different cases of process intensification in the RF operation. For each of these cases, we consider the effect of operating in the three regimes described above. Investigating the reactor conditions for various times into the RF operation allows us to analyze the reactor operation. In the next three subsections, we consider each of the three cases of process intensification: nominal reactor case, shorter 5-cm-reactor case, and the poorly insulated reactor case.

### *Nominal reactor: favorable thermodynamic conditions*

As the first example, we investigate the performance of the microreactor for the base case (case 2 in Table 1). Because the approximate timescales for the reactions are smaller than the advection timescale, the reactions attain equilibrium within the reactor. The rates of oxidation, reforming, and water gas shift at the UD steady state are plotted in Figure 5 with the temperature profile shown in the background as a thick gray line. Most

**Table 2. Simulations of the Reactor Performance for Various Inlet Feed Ratios for Poorly Insulated Reverse-Flow Reactor Case with Switching Time of 5 s**

| Case | $CH_4$:$O_2$ Ratio | $T_{s,\max}$ | $T_{s,\text{out}}$ | %$H_2$ Yield |
|---|---|---|---|---|
| 1 | 0.7:1 | 1598 | 750 | 47.2 |
| 2 | 1:1 | 1566 | 696 | 44.5 |
| 3 | 1.25:1 | 1474 | 634 | 38.0 |
| 4 | 1.5:1 | 1445 | 610 | 31.6 |
| 5 | 2:1 | 1436 | 595 | 25.2 |

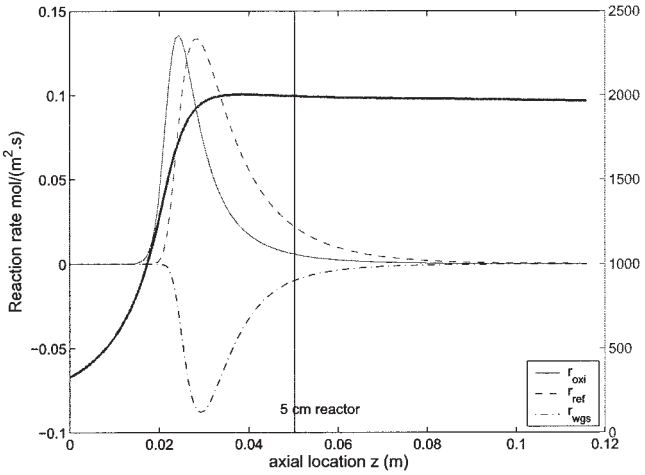


**Figure 5. Reaction rates at the UD steady state for the base case.**

The temperature profile is shown as a thick gray line. Most of the reactions take place about 3.5 cm from the reactor inlet. Profiles for the shorter 5-cm reactor are similar. The vertical line represents the 5-cm mark.

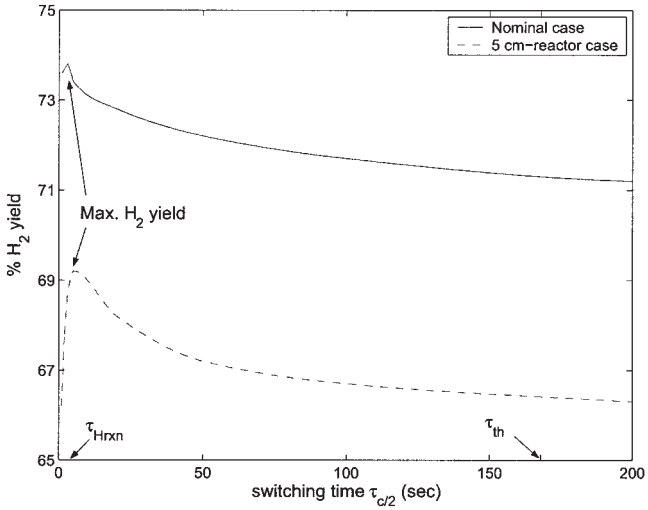


**Figure 7. Hydrogen yield in the RF operation as a function of the switching time for the nominal case and short 5-cm reactor case.**

The maxima observed at $\tau_{c/2} \approx 4$ s corresponds to the timescale of reaction heat release.

of the reactions take place near the maximum temperature, which occurs about 3.5 cm from the reactor inlet, whereas the rest of the reactor is used in reaching equilibrium. The portion of the reactor upstream of this zone is cooled by the incoming stream and virtually goes unused because no reaction occurs there.

Figure 6 shows the temperature profile at various times after the flow reversal for a half-cycle time of $\tau_{c/2} = 200$ s. Immediately after the flow reversal, the temperature at the reactor inlet (outlet in the previous half-cycle) is high, whereas that at the outlet is low. As the time progresses, the temperature at the inlet drops because of the incoming cold feed and that at the outlet increases because of the heat released on reaction and heat transfer from the hot gas flow. The time taken for this is governed primarily by the timescale of solid thermal inertia ($\tau_{th}$) as well as the timescale of reaction heat release ($\tau_{Hrxn}$). At

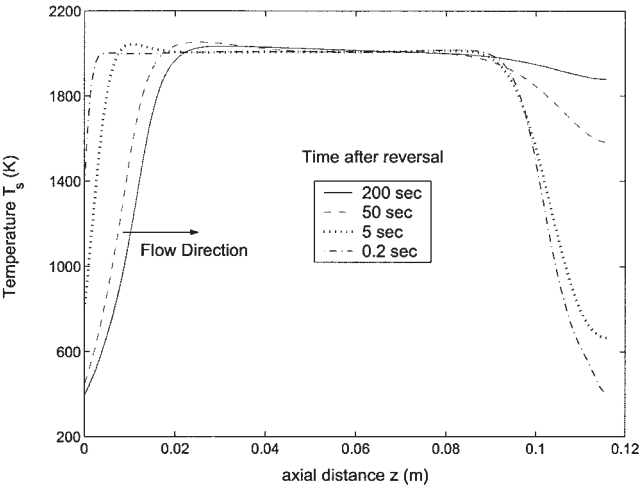


**Figure 6. Temperature profiles at various times after flow reversal in the reactor with switching time of $\tau_{c/2} = 200$ s.**

5 s after the flow reversal (dotted line), which is an order of magnitude lower than $\tau_{th}$, the outlet temperature is still quite low. As the time progresses, the inlet temperature drops and the outlet temperature increases progressively (dashed line: 50 s after flow reversal). At 200 s, which is greater than $\tau_{th}$, the temperature profile is similar qualitatively to the UD steady state. Thus, if the switching time is large (such as $\tau_{c/2} = 200$ s) comparable to $\tau_{th}$, the reactor has enough time to respond thermally to the temperature changes. As a result, the conditions in the RF operation approach that in the UD operation; thus, hardly any change in the hydrogen yield is observed at higher switching times. This is illustrated in Figure 7, where the RF yield asymptotically approaches the UD yield as $\tau_{c/2}$ is further increased beyond $\tau_{th}$.

The temperature profile (thick gray line) and the rates of reactions in the RF operation with a fast switching time of 5 s are shown in Figure 8. A low-temperature region that appears at the reactor end is thermodynamically favorable for the water gas shift (WGS) reaction, resulting in an improved $H_2$ yield. Although low temperature is unfavorable for the endothermic reforming reaction, the equilibrium constant for reforming reaction drops from about $10^6$ to about $10^3$. The equilibrium constant is still high enough to ensure that the reaction essentially proceeds to completion (in the forward direction) and does not adversely affect the $H_2$ yield. We also observe from Figure 7 that as the switching time increases, there is a decrease in the $H_2$ yield, with the optimal switching time in the range 2–5 s. Switching at very high frequencies ($<1$ s) is also undesirable because hydrogen concentration requires some time to respond and attain pseudo-steady state after the port switching.

To ensure that indeed the favorable thermodynamic conditions for WGS reaction were responsible for the observed phenomenon, we simulated the reactor assuming no WGS occurs within the reactor. With WGS "turned off," the $H_2$ yield on the RF operation was similar to that of the UD operation (a

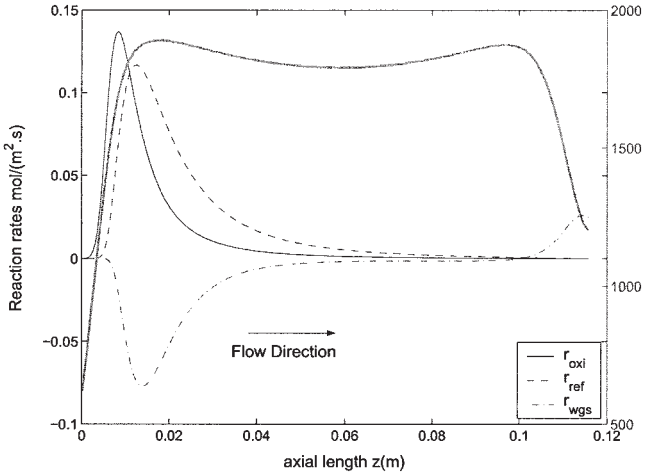


**Figure 8. Rates of reactions and temperature profile (thick gray line) just before port switching (at $t = n\tau_{c/2}$) for a switching time of $\tau_{c/2} = 5$ s.**

High-temperature central region allows reactions to reach equilibrium. Lower temperature at the reactor end favors water gas shift reaction.

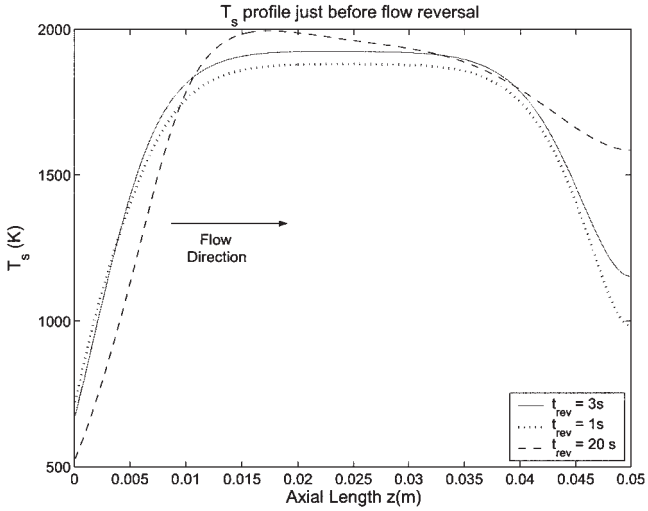


**Figure 10. Temperature profile for various switching times in the 5-cm reactor after attaining periodic steady state.**

small decrease in $H_2$ yield was observed as a result of the reforming reaction).

Another interesting outcome is that the "NK" kinetics model considered in Part 1 of this series[16] could not reproduce the observed differences in the UD and RF operations. Figure 9 shows the rates of WGS: thick lines represent the RF operation; thin lines represent the UD operation; solid lines represent the GOS model; and dashed lines represent the NK model. The rate of WGS reaction in the NK model is an order of magnitude lower than the GOS model. In the RF operation, no significant WGS reaction occurs in the small end region of lower temperature in the reactor (thick, dashed line). As a result, the difference in the UD and RF yields is not significant for the NK model.

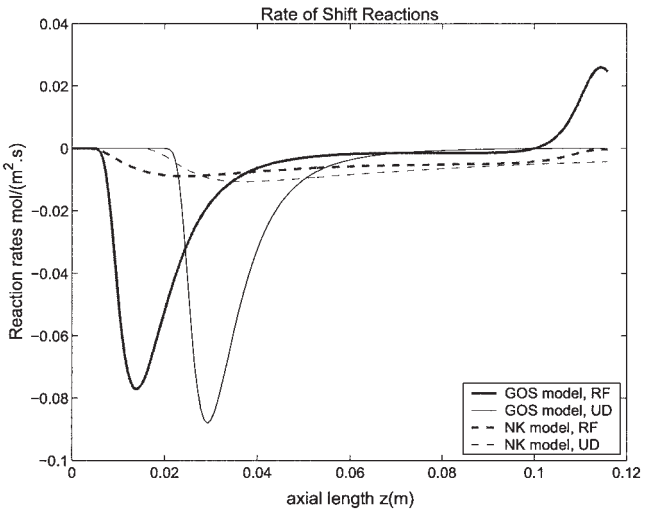


**Figure 9. Rate of water gas shift reaction in the UD (thin lines) and RF (thick lines) operation.**

For the GOS model (—), low $T_s$ at the reactor end favors shift reaction, whereas it is insignificant for NK model (– –).

### *Better thermal utilization in a short reactor*

Figure 7 shows the hydrogen yield for the RF operation in a 5-cm-long reactor as a function of the time of flow reversal. As in the previous case, faster switching in the reactor gives a higher hydrogen yield, whereas the hydrogen yield asymptotically approaches that in the UD operation at greater switching times. A clear maximum is observed at a switching time of about 4 s.

For the shorter reactor, the advection timescale is comparable to that of the reforming reaction. The rates of reactions and temperature profile are similar to those seen in the previous example (Figure 5). The temperature maximum is observed at 3.5 cm from the reactor inlet. Consequently, the reactor length is not sufficient for the reforming and WGS reactions to reach equilibrium. This results in a lower hydrogen yield in the UD operation. Because the temperature peak occurs close to the reactor exit, the entire length of the microreactor is not properly used.

The reverse-flow operation with fast switching results in a more uniform temperature profile at the center of the reactor. Figure 10 shows the temperature profiles within the reactor just before switching of the input and output ports (that is, at $t = n\tau_{c/2}$) for three different switching times of 1 s ($\tau_{c/2} < \tau_{Hrxn}$), 3 s ($\tau_{c/2} \approx \tau_{Hrxn}$), and 20 s ($\tau_{c/2} > \tau_{Hrxn}$). The temperature profile for fast switching time of $\tau_{c/2} = 1$ s is shown as a solid line in the figure. As the switching time is increased, the peak temperature increases, resulting in an increase in conversion to hydrogen. This happens approximately until switching time reaches the timescale of reaction heat release. When the switching time is further increased, the reactor enters a wave development stage,[12] in which a single reactor hotspot is formed and it starts migrating toward the center of the reactor. In this stage, the output hydrogen concentration starts falling because the reforming reaction is unable to proceed to completion as the hotspot approaches its UD steady-state location. Consequently, a maximum in the hydrogen yield is observed at $\tau_{c/2} = 4$ s, which corresponds to the approximate timescale of

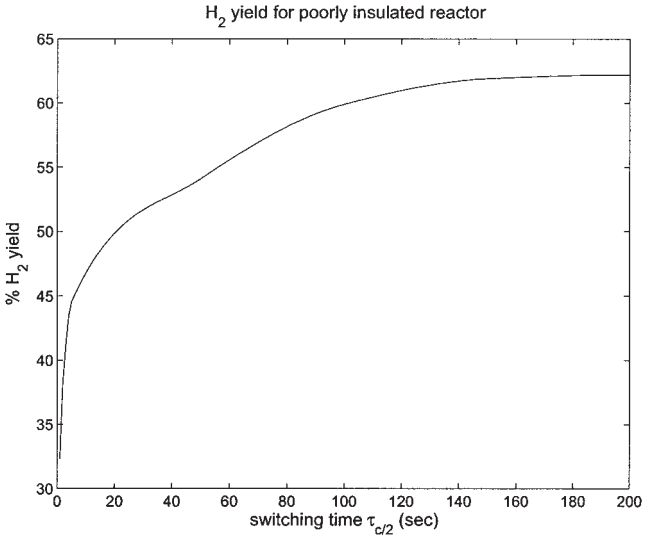


**Figure 11. Hydrogen yield in the RF operation as a function of the switching time with heat loss to the surroundings included.**

Infrequent switching on the scale approaching the timescale for the reactor thermal inertia provides maximum yield for this case.

reaction heat release $\tau_{Hrxn}$, attributed to the optimal thermal use of the reactor.

### *Using reactor as a regenerative heat exchanger*

One of the most widely studied applications of the RF operation is to use the reactor structure as a regenerative heat exchanger to trap a creeping thermal wave within the reactor and maintain autothermal operation in systems where the heat released on reactions is insufficient to maintain autothermal UD operation. This situation was indeed observed in our simulations when the effect of heat loss was included. Fast switching in this case results in significantly lower peak temperatures, resulting from the large heat losses. Consequently, the reactions do not proceed to completion and the hydrogen yield is low. As the switching time is increased, the peak temperature increases, and a thermal wave develops and starts propagating along the length of the reactor. Switching at the wave propagation stage gives the maximum yield. Hydrogen yield is plotted as a function of switching time $\tau_{c/2}$ in Figure 11. Optimum RF performance is obtained as the switching time approaches the timescale of thermal inertia in this case. Increasing the switching time beyond $\tau_{th}$ does not cause any significant increase in hydrogen yield. The maximum limit for switching time is given by the time required for the reaction zone to travel through the reactor, which was found to be about 1200 s for this case.

## Conclusions

Parametric simulation results of autothermal partial oxidation of methane in a microreactor were presented in this paper. It was demonstrated that reverse-flow operation of the reactor provides better hydrogen yields and lower temperatures for most cases considered. An analysis of the observed improvement in the reactor performance in reverse-flow operation over unidirectional operation was presented and approximate guidelines on operating the reverse-flow reactor based on simple timescale analysis were developed. Specific results of this work include:

- The thermal dynamics of the reactor was found to be the dominant effect in this system, which can be exploited through reverse-flow operation.
- The timescale of heat release attributed to reactions was found to be an important parameter for the system. The optimum reactor yield was obtained when the switching time was close to this timescale.
- In addition to some improvements in reactor yields, the main advantages of the reverse-flow operation were lower reactor temperature and robustness of the reactor performance under various operating conditions. The unidirectional autothermal steady state disappeared at higher inlet velocities, higher methane content in the feed, and poor reactor insulation (significant heat losses). However, autothermal operation was maintained in the reverse-flow mode.
- The improvement in the hydrogen yield brought by the RF operation was much greater in the case of the shorter 5-cm-long reactor.
- Three different cases for process intensification in reverse-flow operation were observed in the system.

(1) For the 11.6-cm-long reactor, the improvement in the hydrogen yield occurred because of better thermodynamic conditions at the reactor exit. In this case, fast switching ($\tau_{c/2} = 2$ to 5 s) was found to be optimal.

(2) In the case of the shorter reactor, better thermal utilization was responsible for the improved hydrogen yield. The optimal reactor performance was obtained when the switching time approached the timescale of reaction heat release.

(3) For the large heat loss case, the microreactor was used as a regenerative heat exchanger to trap the traveling thermal wave by flow reversal.

- The RF operation does not guarantee to provide improvements in the hydrogen yield in all cases. For $CH_4$:$O_2$ = 1.25:1 and higher, the unidirectional operation was in fact better than the reverse-flow operation.

## Acknowledgments

The authors gratefully acknowledge Dr. Athanasios Nenes in the School of Chemical and Biomolecular Engineering for his help with the numerical simulations. J.H.L. gratefully acknowledges the financial support from NSF (CTS-0301993). A.G.F. gratefully acknowledges a NASA grant (UG03–0050 NRA 02-OBPR-03, Project Monitor Dr. Karen Weiland) to support this work.

## Literature Cited

1. Matros YS. Forced unsteady-state processes in heterogeneous catalytic reactors. *Can J Chem Eng*. 1996;74:566-579.
2. Horn FJM, Lin RC. Periodic processes: A variational approach. *Ind Eng Chem Des Dev*. 1967;6:21-30.
3. Horn FJM. Periodic countercurrent processes. *Ind Eng Chem Des Dev*. 1967;6:30-36.
4. Sterman LE, Ydstie BE. The steady-state process with periodic perturbations. *Chem Eng Sci*. 1990;45:721-736.
5. Sterman LE, Ydstie BE. Periodic forcing of the CSTR: An application of the generalized pi criterion. *AIChE J*. 1991;37:986-996.
6. Bailey JE. Optimal periodic processes in the limits of very fast and very slow cycling. *Automatica*. 1972;8:451-454.
7. Eigenberger G, Nieken D. Catalytic combustion with periodic flow reversal. *Chem Eng Sci*. 1988;43:2109-2115.

8. Haynes TN, Georgakis C, Caram HS. The design of reverse flow reactors for catalytic combustion systems. *Chem Eng Sci*. 1995;50: 401-416.
9. Matros YS, Bunimovich GA. Reverse-flow operation in fixed bed catalytic reactors. *Catal Rev Sci Eng*. 1996;38:1-68.
10. Matros YS. *Catalytic Processes under Unsteady-State Conditions* (Studies in Surface Science and Catalysis series). Amsterdam: Elsevier; 1989.
11. Blanks RF, Wittrig TS, Peterson DA. Bidirectional adiabatic synthesis gas generator. *Chem Eng Sci.* 1990;45:2407-2413.
12. de Groote AM, Froment GF, Kobylinski TH. Synthesis gas production from natural gas in a fixed bed reactor with reversed flow. *Can J Chem Eng*. 1996;74:735-742.
13. Gosiewski K, Bartmann D, Moszczynski M, Mleczko L. Effect of the intraparticle mass transport limitations on temperature profiles and catalytic performance of the reverse-flow reactor for the partial oxidation of methane to synthesis gas. *Chem Eng Sci*. 1999;54:4589-4602.
14. Gosiewski K. Mathematical simulations of reactors for catalytic conversion of methane to syngas with forced concentration cycling. *Chem Eng Process.* 2000;39:459-469.
15. Fissore D, Barresi AA, Baldi G. Synthesis gas production in a forced unsteady-state reactor network. *Ind Eng Chem Res.* 2003;42:2489-2495.
16. Kaisare NS, Lee JH, Fedorov AG. Hydrogen generation in a reverse-flow microreactor: 1. Model formulation and scaling. *AIChE J.* 2005; 00;000-000.
17. Kikas T, Bardenshteyn I, Williamson C, Ejimofor C, Puri P, Fedorov AG. Hydrogen production in a reverse-flow autothermal catalytic microreactor: From evidence of performance enhancement to innovative reactor design. *Ind Eng Chem Res*. 2003;42:6273-6279.

*Manuscript received Aug. 24, 2004, and revision received Dec. 9, 2004.*